Composites Science and Technology
October 2017, Volume 151, Pages 228-233
http://dx.doi.org/10.1016/j.compscitech.2017.08.028
http://archimer.ifremer.fr/doc/00397/50830/

Hygroscopic expansion: A key point to describe natural fibre/polymer matrix interface bond strength

le Duigou Antoine [1, *], Merotte Justin [1, 3], Bourmaud Alain [1], Davies Peter [2], Belhouli Karim [3], Baley Christophe [1]

[1] Polymer and Composites, Univ. Bretagne Sud, FRE CNRS 3744, IRDL, France
[2] Ifremer, Marine Structures Group, Centre de Bretagne, BP 70, 29280, Plouzané, France
[3] EcoTechnilin SAS, F-76190, Valliquerville, France

* Corresponding author : Antoine le Duigou, email address : antoine.le-duigou@univ-ubs.fr

Abstract :

The present article aims to investigate the contribution of hygroscopic expansion of flax fibres to interfacial radial stresses and Interfacial Shear Strength (IFSS) of Maleic Anhydride grafted PolyPropylene (MAPP)/Flax biocomposites.

During manufacturing of thermoplastic biocomposites and storage at 50% RH, a weight variation is observed, attributed to water content evolution within plant cell-walls. The hygroscopic radial expansion coefficient βr flax of single flax fibres estimated by Environmental Scanning Electron Microscopy (ESEM) observation is many orders of magnitude higher (βf,R = 1.14 ε/Δm) than thermal expansion (αf, R = 78 10−6 ε/°C). Thus, its contribution to the development of residual stresses σrad during processing should be prevalent. A multiscale analysis of interfacial stress state and hygroscopic contribution is performed with the use of a cylindrical concentric model at microscopic scale and asymmetric composite laminates [0, 90°] curvature generation at macroscopic scale. Similar radial stresses are obtained, while relevant values of μ (IFSS/σrad) ≈ 0.46 are calculated. Therefore, the interfacial bond strength of natural fiber/polymer systems should be described by taking into account their hygroscopic behavior.

Keywords : Flax fibres, Fibre/matrix bond

1. Introduction

Interfacial bond strength in fibre/matrix composite systems is typically produced by several complex mechanisms such as mechanical anchorage, chemical bonding, interdiffusion and so on. For thermoplastic polymer where low chemical bonding is expected, residual stresses that arise from thermal mismatch between components ($\Delta\alpha$) make a major contribution to interfacial bond strength [1] [2].

Bast fibres such as flax are increasingly used for composite reinforcement due to their high specific stiffness [3]. However, the natural fibre/polymer interfacial bond strength is often considered as a limitation for biocomposites. Thomason *et al* [4] suggest that fibre anisotropy and high thermal radial expansion lower thermal mismatch and interfacial shear strength. Indeed, plant fibres such as flax exhibit 15 times higher transverse thermal expansion coefficients than glass fibres ($\alpha_{fL\ flax}$ = 2.8 10^{-6}/°C; $\alpha_{fT\ flax}$ = 78 10^{-6}/°C [5] and $\alpha_{fT\ glass}$ = 5 10^{-6}/°C [5]). Similar ideas were proposed by Morgan *et al* [6] to explain low IFSS with Kevlar fibres for which the thermal expansion coefficient is 10 times lower than that of glass ($\alpha_{fT\ kevlar}$= 50 10^{-6}/°C [5]).

However, numerous studies using microbond tests have underlined that plant fibres show satisfactory IFSS levels with PLA [7][8][9][10], PA11 [11], Epoxy [12] or

Polyester [13] with a high contribution of frictional stress and thus residual stresses after debonding [11][10].

Basically, the static friction coefficients μ, obtained from the ratio between interfacial tangential stress (IFSS) and normal stress (radial residual stress) is expressed by a combination of a molecular adhesion component of the frictional force and a deformation component caused by the introduction of microroughness [14].
From previous calculations based on a micromechanical analysis [11], the static friction coefficient μ for PA 11/flax systems was found to give an anomalous value of 5.5 when only thermal residual stresses were taken into account. A similar result has been published by Thomason *et al* [15] on glass epoxy/systems while expected values should be around 0.5 [16] [17]. Thomason et al [15] have shown that when cure shrinkage stresses are added to residual thermal values to describe residual stresses, μ reaches more realistic values around 0.6.This underlines that a complete description of residual stress sources is essential. Thus, for the present work, the IFSS of plant fibres in composites does not to appear to be correctly described by thermal expansion alone, and other sources of residual stresses should be investigated.

Experimental techniques to estimate residual stresses have been reviewed by Parlevliet *et al* [18]. Among them, asymmetric laminates provide a simple indirect indication of residual stress by out-of-plane deformation i.e. warpage. Such laminates have been used for example to reveal hygrothermal [19] and curing stresses [20]. For natural fibres, during water immersion, curvature of asymmetric flax/PP laminates has been observed so that hygroscopic radial stresses around fibres were highlighted [21][22]. Almgren *et al*. claim that hygroscopic stresses could enhance IFSS [23].

The purpose of the present article is to evaluate the contribution of hygroscopic expansion of flax fibres on IFSS as previously only the thermal contribution was taken into account in the literature. First, water content within flax fibres will be monitored throughout the manufacturing and storage steps by gravimetric measurements. Then, hygroscopic coefficient $\beta_{r,\ flax}$ of a single flax fibre will be evaluated using ESEM measurements together with sorption isotherms from the literature. A multiscale evaluation of radial stresses and the contribution of the hygroscopic radial stress will be made. At the microscopic scale, residual stresses (thermal and hygroscopic) will be evaluated by a micromechanical approach based on a concentric cylinder model of transversally isotropic materials. A static friction coefficient μ will subsequently be calculated to validate the assumptions. At macroscopic scale, residual stresses will be investigated by recording the curvature evolution of asymmetric biocomposite laminates curvature after manufacturing and storing. Finally, a novel scenario will be discussed to explain natural fibre/matrix adhesion mechanisms.

2. Material and Methods

2.1 Materials

Biocomposites samples were manufactured with an unidirectional flax tape, 200 g/m² (from Lineo®). Dew retted stems were mechanically scutched and hackled before being processed as a fibrous preform. The supplier claims that no treatment (chemical or physical) has been applied on these fibres. Polypropylene (PP) (PPC 3660 from Total Petrochemicals) and compatibilized PP with 4% PP grafted maleic anhydride (MAPP) (Arkema Orevac CA 100) were extruded and film-cast.

2.2 Composite manufacturing

A stack of polymer films (PP + MAPP) and unidirectional flax-fibre tapes were prepared in a metallic mold (13 x 13 cm²). Unidirectional plies (0 and 90°) and asymmetric laminates [0_3; 90_3] were manufactured. The thicknesses of longitudinal and transverse plies were similar providing an overall laminate thickness of 434 ± 7 µm after processing.

Biocomposites were manufactured with a dedicated hot pressing protocol, holding 190°C for 8 min with an incremental applied pressure up to 20 bar in order to maintain the fibre alignment. The cooling ramp was set to 15°C/min in order to generate moderate residual stresses. The nominal flax fibre volume fraction was 60 %. Biocomposites plates were then cut to provide strips (70x10 mm²) for curvature measurements.

2.3 Gravimetric measurements

Flax fibre preforms and MAPP films were weighed on a 10^{-4} g precision scale prior to processing. To determine initial water content, flax fibres were dried under vacuum at 105°C during 72 H. Weight variation was then measured on asymmetric biocomposites immediately after molding and during storage until constant weight was reached. Water content in flax fibres was determined knowing the initial fibre weight fraction in the composite and assuming that PP and MAPP were insensitive to water.

2.4 Characterization of mechanical properties

The tensile properties of biocomposites with flax fibre orientations set at 0° (E_L) and 90° (E_T) were measured separately on a MTS Synergie™ RT/1000 test machine at

controlled temperature (23°C) with a crosshead displacement speed of 1 mm/min. An axial extensometer with a gauge length of 25 mm (L_0) was used to measure the strain.

2.5 Curvature characterization

The bending curvature of asymmetric biocomposite strips after manufacturing was estimated by periodically taking pictures of one side of a clamped sample. Clamping length was reduced as much as possible (≈ 2 mm) to diminish the effect on stress estimation. The strip geometry (10 mm wide) was selected to reduce bifurcation effects as the thickness-to length ratio and the width-to-length ratio determine the final shape of the laminate [24].

Image analysis was performed using ImageJ® software (National Institutes of Health, USA). The curvature was measured by fitting the time-evolution of the sample to a 'circle' function. Bending curvature (K) was calculated from the radius of the fitted circle.

2.6 ESEM observation

Environmental scanning electron microcopy (FEI) was used to measure flax fibre diameter variation as a function of relative humidity. In environmental mode, vapour pressure range was around 5-10 millibar and measurements were made at room temperature.

For each relative humidity (20-98%), 5 single flax fibres were observed. Fibre diameter was measured at 3 different locations along the fibre and the results were then averaged. The swelling/ shrinkage coefficient β is defined as the strain ε induced by a variation of 1% of moisture content Δm.

3. Results and Discussion

3.1 Weight variation and hygroscopic expansion coefficient

Flax fibres contain 10.3 ± 1 % of water in ambient conditions (T= 23°C and RH = 50%). This water content evolves during the manufacturing step of thermoplastic biocomposites. On 60%-vol flax/MAPP biocomposites, a weight reduction of 50% has been measured between initial preparation and the end of hot compression (Figure 1a). Weight variation is assumed to be only due to water transfer (evaporation and condensation) within the flax fibres as the MAPP matrix is very apolar.

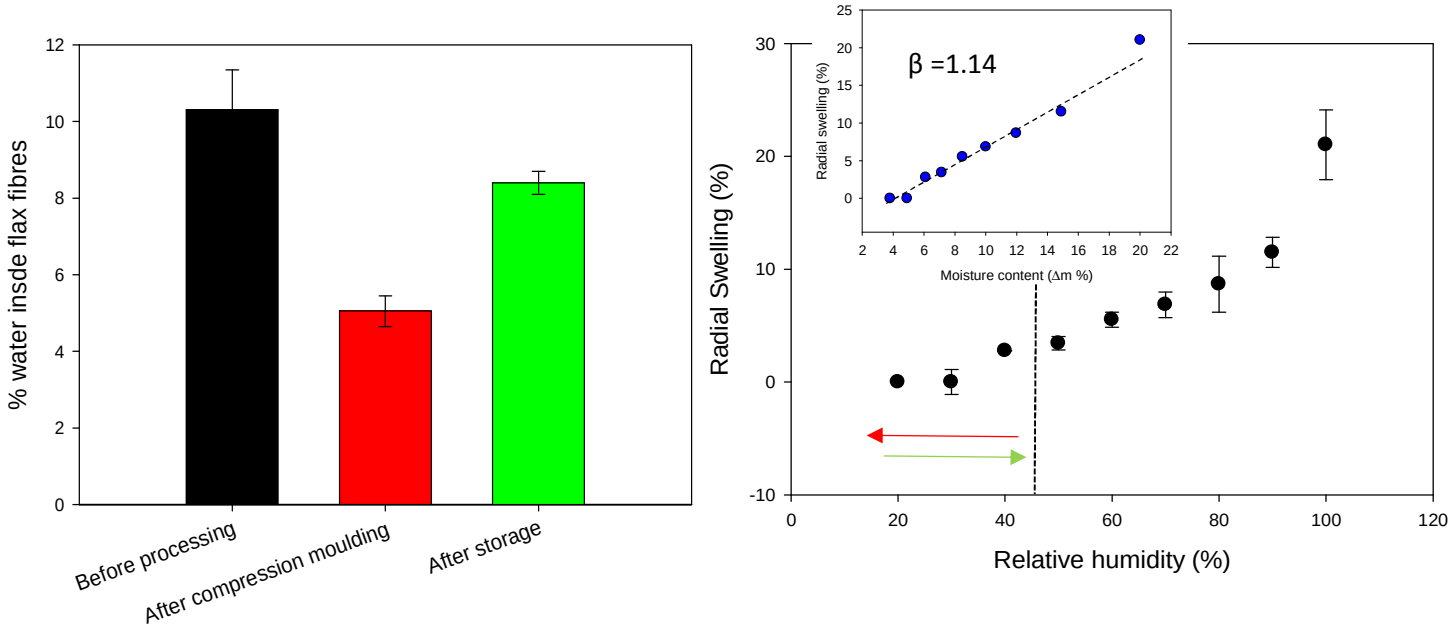

Figure 1 Evolution of water content within flax fibres during compression moulding and storage (T =23°C and RH= 50% during 7200 min) (a), Evolution of radial swelling of a single flax fibre as a function of relative humidity (b) Dotted line indicates the border of the relative humidity during the process, Insert : Evolution of radial swelling as a function of moisture content (from sorption isotherm [25]**)**

Thus, during compression molding (heating and cooling), there is a rise of temperature to 190°C during 8 minutes, a subsequent reduction of relative humidity in the

processing tool and applied pressure, which combine to remove water from the flax fibres. The amount of water inside the biocomposite is then 5.05 ± 0.38 % while fibre shrinkage occurs (Figure 1a). After 7200 minutes (5 days) of storage at 23°C and 50% RH, the water content within the biocomposite increases to reach a constant value of 8.44 ± 0.27% (Figure 1a) while thickness increases by 3.5± 1.8%. Radial swelling of embedded fibres occurs even if they do not recover their initial water content (Figure 1a). A hornification mechanism could partially explain this observation as already observed for flax fibres [26][27]. Indeed, when water is extracted from polysaccharides above a certain level, hydrogen bonds linking water to polysaccharides are disrupted and then rebuild within the polysaccharides. The consequence is a reduction of available hydroxyl groups and thus water sensitivity. Moreover, the surrounding matrix and its constraining effect on flax fibres reduce their accessibility to water but also their swelling [28][29]. The stress state at the fibre/matrix interface is likely to be modified while additional compressive stresses develop on fibres.

As observed in figure 1b, the radial swelling strain of flax fibre reaches a maximal value of 21 ± 3% at 98% RH confirming results of Stuart *et al*. [30] and Pucci *et al.* [31]. Unlike the radial swelling evolution of flax fibre, over the relative humidity scale (20-98 %), its evolution with moisture content (data taken from [25]) appears quasi-linear (R^2= 0.99). Thus, a linear regression enables the radial hygroscopic coefficient $\beta f,_R$ = 1.14 $\varepsilon/\Delta m$ to be estimated for a single flax fibre. Potential underestimation could be argued as ESEM measurements were performed at fibre scale while Dynamic Vapor Sorption (DVS) experiments were conducted at bundle scale [25]. Indeed pectin cements constituting middle lamellae and bundle cohesion are well known to promote water sorption [32]. Comparison with published data should be taken with caution as

only wood fibres have been characterized and modelled. As they possess a larger lumen and a higher lignin content, which should influence swelling, wood fibres exhibit lower $\beta f,_R \approx 0.3\ \varepsilon/\Delta m$ [33] and $0.45\ \varepsilon/\Delta m$ [34]. However, an increase of hemicellulose hygroexpansion in the calculation strongly increases the hygroexpansion that reaches $\beta_{f,R} = 1\ \varepsilon/\Delta m$ for a similar microfibrillar angle [35]. This trend could be assumed to be relevant for flax fibres, which possess a larger amount of pectins and hemicellulose (Galactanes) than wood fibres.

Analyzing the different flax fibre expansion coefficients reveals that the hygroscopic effect is greatly superior to the thermal contribution (table 1).

Table 1 Radial thermal and hygroscopic expansion coefficients of flax single fibre compared to polypropylene

	Single flax fibre	Polypropylene
Radial thermal expansion coefficient $\alpha_{f,T}$ (10^{-6} /°C)	78 [36]	120 [4]
Radial hygroscopic expansion coefficient $\beta_{f,R}$ ($\varepsilon/\Delta m$)	1.14	-

3.2 Multiscale evaluation of hygroscopic radial stress

Evaluation of residual stresses with thermal and hygroscopic contributions is first performed at microscopic scale using a concentric cylinder model of transversally isotropic materials [37]. This model enables interfacial longitudinal and radial stresses to be calculated, including both the anisotropic properties of fibres and the thermal

strain effects. Thermal strain describes the strain incompatibility between fibre and matrix as:

$$\varepsilon_{thermic} = (\alpha_{f(L,R)} - \alpha_m)\Delta T \qquad \text{Equation 1}$$

With α the thermal expansion of fibre and matrix. L and R are longitudinal and radial directions. ΔT is the temperature range over which thermal stresses are locked. For thermoplastic polymers, crystallization temperature is currently used [38]. For the MAPP matrix used here, T_c = 110°C. Input data are taken from Table 1 and E_{fL} = 55000 MPa [3], E_{fT} = 7000 MPa [39].

The thermal radial stress obtained for MAPP/flax is $\sigma_{rad\ Thermal}$= -3.65 MPa. This negative value can be explained by the higher value of α_m compared to α_{fT} and α_{fL} and means that a compressive state occurs in the fibre/matrix interface area. These values are close to those published elsewhere on PA11/Flax [11] and PP/jute [4].

Determination of the static friction coefficients μ, obtained from the ratio between interfacial tangential stress (IFSS) and normal stress (radial residual stress) evaluated by eq 2. provide values around 0.65 for glass/PP [16] and 0.6 for carbon/epoxy [17].

$$\tau_{app} = \mu . \sigma_{Residual} \qquad \text{Equation 2}$$

Using τ_{app} for MAPP/flax of 10.6 ± 2.7 MPa [40] and $\sigma_{residual}$= 3.4 MPa leads to an anomalous value of μ = 3.11. This high value of μ (> 1) can be attributed to a missing source of residual stress [15].

As shown in Figure 1b and in Table 1, hygroscopic expansion of flax fibres is significantly higher than their thermal expansion. Thus, radial stress can be calculated using the Wagner and Nairn model [37] where thermal strains are substituted by hygroscopic strain:

$$\varepsilon_{hygro} = (\beta_{f(L,R)} - \beta_m)\Delta m \qquad \text{Equation 3}$$

With β the hygroscopic expansion of fibre and matrix. L and R are longitudinal and radial directions. $\beta_{f,\,L}$ has not been measured here but is assumed to be close to zero similarly to wood fibres [33]. β_m for MAPP is also assumed to be negligible and Δm is the moisture content difference between the end of compression moulding and storage, i.e. 3.4%. The stiffness of flax fibres and MAPP are assumed to be constant over such a moisture content range [41]. Thus, $\sigma_{rad,\,hygrosocpic}$ = 26.7 MPa. Calculating the overall radial stress as the addition of the contribution of the tensile hygroscopic stress $\sigma_{rad\ hygroscopic}$ to the compressive thermal value $\sigma_{rad\ thermal,}$ leads to $\sigma_{global} = \sigma_{rad\ hygroscopic} + \sigma_{rad\ thermal,}$ = 26.7 – 3.65 = 23.05 MPa.

Validation is then performed by calculating the static friction coefficient μ (Eq. 2) which reaches 0.46 and matches very well those of other systems such as PP/glass [16] and Epoxy/glass [17]. Thus, hygroscopic strains could be considered as the missing source that needs to be taken into account in evaluating the IFSS of natural fibre systems.

Microscopic evaluation of σ_{rad} by a micromechanical model was performed on an idealized cylinder geometry with very low fibre content ($v_f \approx 1\%$) [42]. Therefore, asymmetric biocomposites laminates [0_3/ 90_3] were also used, to assess the development of residual stresses at the macroscale.

Once the compression molding step is finished, these biocomposites show a significant curvature due to the thermal expansion and hygroscopic shrinkage of 90° oriented plies (Figure 2). After 5 days of storage at 50% RH and ambient temperature, the curvature of the biocomposite reaches a stationary position (Figure 2) with a slightly inversed

curvature. Stress released by creep mechanisms is assumed to be negligible during this time period.

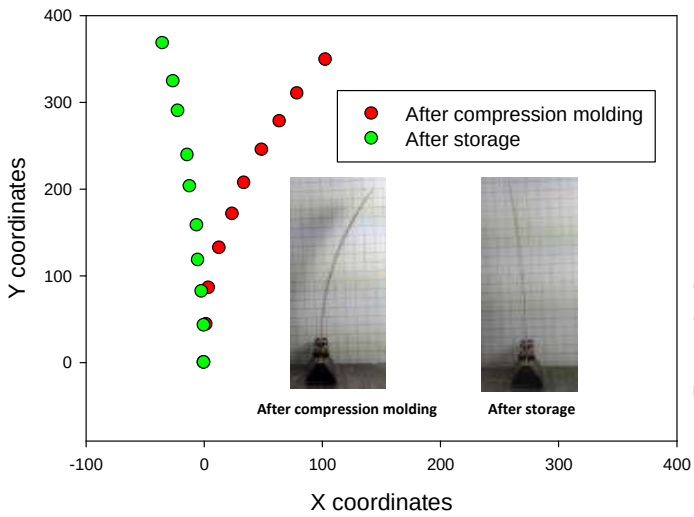

Figure 21 Evolution of asymmetric biocomposite laminate [0_3/ 90_3] curvature after compression molding and storage at room temperature and RH =50%. (For interpretation of the references to color in this figure legend, the reader is referred to the web version of this article)

Residual stresses generated during processing and during storage could be estimated separately from the curvature value at each step using equation 4 [43]:

$$\sigma_{22} = \sigma_{radial} = \frac{E_{11}.E_{22}}{E_{11}+E_{22}}\frac{t}{\Delta\rho}\left(\frac{1}{2}+\frac{1}{24}(2+\frac{E_{11}}{G_{12}}+\frac{E_{22}}{G_{12}}\right) \qquad \text{Equation 4}$$

With t the thickness of the sample (t= 0.450mm), $\Delta\rho$ the differential curvature radius ($\Delta\rho_{\text{after compression}}$ = 154.3 ± 18 mm; $\Delta\rho_{\text{after storage}}$ = 126 ± 12 mm), E_{11} and E_{22} are the values of longitudinal modulus (E_{11} =30950 ± 2107 MPa) and transverse modulus (E_{22} = 1791 ± 180 MPa), G_{12} is the in-plane shear modulus estimated by rule of mixture giving G_{12} = 1041 MPa using G_{flt}= 2500 MPa [44] and $G_m = \frac{\sigma_m}{2(1+\vartheta)}$ with σ_m = 1500 ± 100 MPa. No significant difference of mechanical properties of the composite is assumed between the end of compression and the end of storage.

Consequently, the radial stress developed during compression molding is the sum of thermal and hygroscopic contributions and reaches a value of 9.3 ± 0.8 MPa. Storage at 50% RH generates stress of 11.3 ± 1.1 MPa due to hygroscopic expansion of flax fibres. Calculation of the overall residual stress is therefore the sum of both contribution and is 20.6 MPa which is in a similar range to the values obtained by micromechanical modelling.

4-Discussion

A scenario is proposed to describe the contribution of different residual stresses in natural fibre/thermoplastic polymer system that control the interfacial shear strength (Figure 3).

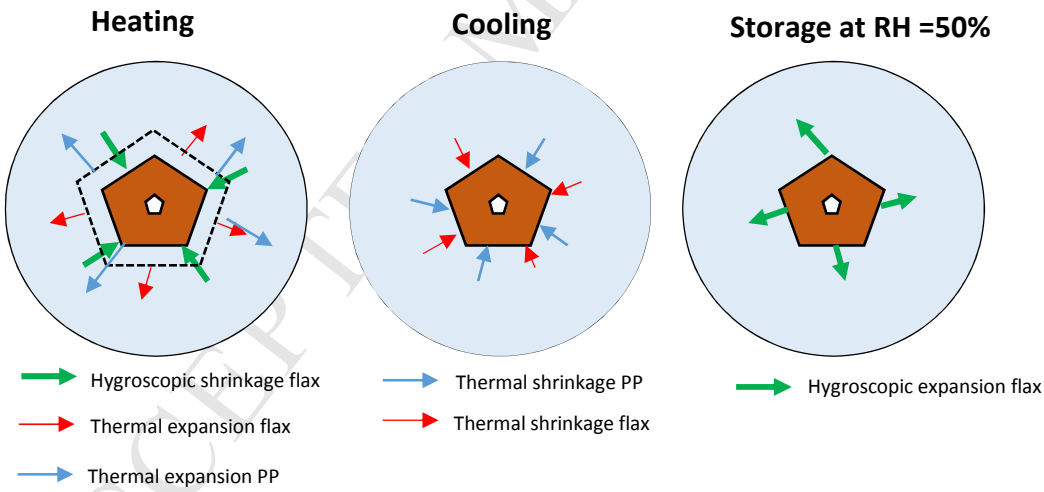

Figure 3 Principle of residual stress generation at plant/matrix interface. Thickness of arrow proportional to the magnitude of stress (For interpretation of the references to color in this figure legend, the reader is referred to the web version of this article)

During processing, flax fibres will mainly shrink due to water evaporation rather than expand thermally. During compression molding, viscous polypropylene matrix will fill

all interstices of the biocomposite. During the cooling step, fibre and matrix will shrink to different extents according to their thermal expansion coefficients. Thermal and hygroscopic stresses will be generated at the fibre/matrix interface. During storing at 50% RH, flax fibres will swell to a larger extent than the matrix. Hygroscopic stress will be produced.

As shown in Table 1 $\alpha_{f, L, R}$ is lower than α_m which yields an initial compressive stress state which is reduced when temperature increases [1]. As $\beta_{f, L, R}$ is much higher than β_m, $\alpha_{f, L, R}$ and α_m, an initial tensile stress state will appear at the fibre /matrix interface. Drying these materials after processing will therefore reduce the radial stresses, while increasing humidity and moisture content will increase radial stress and thus raise IFSS, to a limit that is still unknown.

5- Conclusion

The present article has shown that during manufacturing and storage of thermoplastic biocomposites, a weight variation is observed, attributed to a modification of water content in the composite and thus in flax fibres. The hygroscopic radial expansion coefficient of flax fibre has been estimated and it is many orders of magnitude higher than the thermal expansion.

Estimation of residual stress using only thermal strain is not correct, as the static friction coefficient reaches an anomalous value of 3.11. Taking the hygroscopic strain into account, results in the residual stresses increasing significantly, from -3.65 to 23.05 MPa which may lead to damage mechanism. Including the overall residual stress in the calculation of μ leads to a more satisfactory value of 0.46.

As micromechanical modelling and an experimental approach converge to a similar and more relevant value of static friction coefficient, the hygroscopic behavior of natural

fibres must be added to the thermal response in order to describe their interfacial performance correctly. For natural fibres and flax for instance, the high contribution of hygroscopic stress due to flax fibre expansion controls the stress state at the fibre/matrix interface and thus the performance.

This information provides a new insight into the plant fibre/matrix interface bonding mechanism. Indeed, initially considered as a drawback, the moisture sensitivity of flax fibres could be turned into an advantage if radial stress can be generated. In this context, the benefits of reducing their water affinity by different kinds of treatments appear to be questionable. From an industrial point of view, the effect of a degassing that releases a large amount of water may be of interest for further study as it may amplify the swelling of plant fibres.

6- References

[1] Thomason JL, Yang L. Temperature dependence of the interfacial shear strength in glass–fibre polypropylene composites. Compos Sci Technol 2011;71:1600–5. doi:10.1016/j.compscitech.2011.07.006.

[2] Dzral L. The bonding mechanism of aramid fibres to epoxy matrices - Part 1 A review of the literature. J Mater Sci 1990;25:4186–93.

[3] Baley C, Bourmaud A. Average tensile properties of French elementary flax fibers. Mater Lett 2014;122:159–61. doi:http://dx.doi.org/10.1016/j.matlet.2014.02.030.

[4] Thomason J. Dependence of interfacial strength on the anisotropic fiber properties of jute reinforced composites. Pollymer Compos 2009;31.

[5] Gentles F, Anderson J, Thomason J. Characterisation of the transverse thermoelastic properties of natural fibres used in composites. 14th Eur. Conf. Compos. Mater. ECCM14, 2010, p. http://strathprints.strath.ac.uk/27074/1/strathpri.

[6] Morgan RJ, Pruneda CO SW. The relationship between the physical structure and the microscopic deformation and failure processes of poly(para-phenylene terephtalamide) fibers. J Polym Sci Pt B-Polym Phys 1983;21:1757–83.

[7] le Duigou A, Bourmaud A, Balnois E, Davies P, Baley C. Improving the interfacial properties between flax fibres and PLLA by a water fibre treatment and drying cycle. Ind Crops Prod 2012;39:31–9. doi:10.1016/j.indcrop.2012.02.001.

[8] Le Duigou A, Davies P, Baley C. Interfacial bonding of Flax fibre/Poly(l-lactide) bio-composites. Compos Sci Technol 2010;70:231–9. doi:10.1016/j.compscitech.2009.10.009.

[9] L. Yang JLT. Development and application of micromechanical techniques for characterising interfacial shear strength in fibre-thermoplastic composites. Polym Test 2012;31:895–903.

[10] Graupner N, Rößler J, Ziegmann G, Müssig J. Fibre/matrix adhesion of cellulose fibres in PLA, PP and MAPP: A critical review of pull-out test, microbond test and single fibre fragmentation test results. Compos Part A Appl Sci Manuf 2014;63:133–48. doi:http://dx.doi.org/10.1016/j.compositesa.2014.04.011.

[11] Le Duigou A, Bourmaud A, Gourier C, Baley C. Multi-scale shear properties of flax fibre reinforced polyamide 11 biocomposites. Compos Part A Appl Sci

Manuf 2016;85:123–9. doi:10.1016/j.compositesa.2016.03.014.

[12] Le Duigou A, Kervoelen A, Le Grand A, Nardin M, Baley C. Interfacial properties of flax fibre–epoxy resin systems: Existence of a complex interphase. Compos Sci Technol 2014;100:152–7. doi:10.1016/j.compscitech.2014.06.009.

[13] Baley C, Busnel F, Grohens Y, Sire O. Influence of chemical treatments on surface properties and adhesion of flax fibre–polyester resin. Compos Part A Appl Sci Manuf 2006;37:1626–37. doi:10.1016/j.compositesa.2005.10.014.

[14] Mikhin NM AN. dependence of the coefficient of external static friction on temperature. Investig Sov Phys J 1974;17:873–5.

[15] J.L. Thomason, Yang L. Temperature dependence of the interfacial shear strength in glass–fibre epoxy composites. Compos Sci Technol 2014;96:7–12.

[16] G.E. Schoolenberg. Polypropylene: structure, blends and composites. J Karger-Kocsis (Ed), Chapmann Hall [Chapter 36] n.d.

[17] M. Detassis, A. Pegoretti CM. Effect of temperature and strain rate on interfacial shear stress transmission in carbon/epoxy model composites. Compos Sci Technol 53AD;1995:39–46.

[18] Parlevliet P, Bersee H and BA. Residual stresses in thermoplastic composites--A study of the literature--Part I: Formation of residual stresses. Comp Part A Appl Sci Manuf 2006;37:1847–57.

[19] M Gigliotti, F Jacquemin, Vautrin A. Assessment of approximate models to evaluate transient and cyclical hygrothermoelastic stress in composite plates. Int J Solids Struct 2007;44:733–59.

[20] M. Gigliotti, M.R. Wisnom KDP. Development of curvature during the cure of AS4/8552 [0/90] unsymmetric composite plates. Compos Sci Technol 2003;63:187–97.

[21] Le Duigou A, Castro M. Moisture-induced self-shaping flax-reinforced polypropylene biocomposite actuator. Ind Crops Prod 2015;71:1–6. doi:10.1016/j.indcrop.2015.03.077.

[22] Le Duigou, A., Castro M. Hygromorph BioComposites : Effect of fibre content and interfacial strength on the actuation performances. Ind Crop Prod 2017;99:142–9.

[23] Almgren KM, Gamstedt EK. Characterization of Interfacial Stress Transfer Ability by Dynamic Mechanical Analysis of Cellulose Fiber Based Composite Materials. Compos Interfaces 2010;17:845–61. doi:10.1163/092764410X539235.

[24] Jeronimidis G PA. Residual-stresses in carbon fiber– thermoplastic matrix laminates. J Compos Mater 1988;22:401–15.

[25] Hill CAS, Norton A, Newman G. The water vapor sorption behavior of natural fibers. J Appl Polym Sci 2009;112:1524–37. doi:10.1002/app.29725.

[26] Diniz J. M. B. F., Gil M. H. CJ a. a. M. Hornification—its origin and interpretation in wood pulps. Wood Sci Technol 2004;37:489–94.

[27] Gourier C, Le Duigou A, Bourmaud A, Baley C. Mechanical analysis of elementary flax fibre tensile properties after different thermal cycles. Compos Part A Appl Sci Manuf 2014;64:159–66. doi:10.1016/j.compositesa.2014.05.006.

[28] Le Duigou A, Castro M. Evaluation of force generation mechanisms in natural,

passive hydraulic actuators. Sci Rep 2016;18105.

[29] Joffre T, Wernersson ELG, Miettinen A, Luengo Hendriks CL, Gamstedt EK. Swelling of cellulose fibres in composite materials: Constraint effects of the surrounding matrix. Compos Sci Technol 2013;74:52–9. doi:10.1016/j.compscitech.2012.10.006.

[30] Stuart T, McCall RD, Sharma HSS, Lyons G. Modelling of wicking and moisture interactions of flax and viscose fibres. Carbohydr Polym 2015;123:359–68. doi:10.1016/j.carbpol.2015.01.053.

[31] MF Pucci, PJ Liotier SD. Capillary wicking in flax fabrics – Effects of swelling in water. Colloids Surfaces A Physicochem Eng Asp 2016;498.

[32] Martin N, Davies P, Baley C. Comparison of the properties of scutched flax and flax tow for composite material reinforcement. Ind Crops Prod 2014;61:284–92. doi:10.1016/j.indcrop.2014.07.015.

[33] Joffre T, Neagu RC, Bardage SL, Gamstedt EK. Modelling of the hygroelastic behaviour of normal and compression wood tracheids. J Struct Biol 2014;185:89–98. doi:10.1016/j.jsb.2013.10.014.

[34] T. Joffre, P. Isaksson, P.J.J. Dumont, S.Rollanddu Roscoat SS, Gamstedt LO& EK. A Method to Measure Moisture Induced Swelling Properties of a Single Wood Cell. Exp Mech 2016.

[35] E Marklund JV. Modeling the hygroexpansion of aligned wood fiber composites. Compos Sci Technol 2009;69:1108–14.

[36] Cichocki Jr. FR, Thomason JL. Thermoelastic anisotropy of a natural fiber.

Compos Sci Technol 2002;62:669–78.

[37] H. D. Wagner & J. A. Nairn. Residual thermal stresses in three concentric transverselty isotropic cylinders: Application to thermoplastic-matrix composites containing a transcrystalline interphase. Compos Sci Technol 1997;57:1289–302.

[38] J.A. Nairn PZ. Matrix solidification and the resulting residual thermal stresses in composites. J Mater Sci 1985;20:355–67.

[39] Baley C, Perrot Y, Busnel F, Guezenoc H, Davies P. Transverse tensile behaviour of unidirectional plies reinforced with flax fibres. Mater Lett 2006;60:2984–7. doi:10.1016/j.matlet.2006.02.028.

[40] J Merotte A le Duigou, A. Kervoelen, A. Bourmaud, K. Behlouli, O. Sire and CB. Influence of fibre/matrix interface bond and fibre properties on non-woven vegetal fibre composites. Comp Part A Appl Sci Manuf n.d.

[41] Thuault A, Eve S, Blond D, Gomina M, Breard J. Effects of the hygrothermal environment on the mechanical properties of flax fibres. J Compos Mater 2014;48:1699–707.

[42] L.Yang JLT and. Temperature dependence of the interfacial shear strength in glass–fibre epoxy composites. Compos Sci Technol 2014;96:7–12.

[43] PP. Parlevliet , HE.N. Bersee, AB. Residual stresses in thermoplastic composites—A study of the literature—Part II: Experimental techniques. Comp Part A Appl Sci Manuf 2007;38:651–5.

[44] Baley C Kervoëlen A Le Duigou A Goudenhooft C Bourmaud A. Is the low shear modulus of flax fibres an advantage for polymer reinforcement? Mater Lett

2016;185:534–6.